Determining the Depth and Location of Buried Pipeline by Magnetometer Survey

Chau K. Vo‡, David M. J. Cowell, C. Cookson and S. Freear

School of Electronic and Electrical Engineering, University of Leeds, UK.

S. G. H. Staples

Open University Associate Lecturer, Open University, Milton Keynes, UK.

B. T. H. Varcoe

Experimental Quantum Information, School of Physics & Astronomy, University of Leeds, UK.

E-mail: `c.vo@leeds.ac.uk`

Abstract. This paper proposes a new approach to determine the depth and location of buried pipelines using the remote magnetic field measured by above-ground magnetometer surveys. Calculation is presented and verified by the experimental results on 152-mm (6-in.) steel vessels. Performance of the technique is also evaluated through field trials against industrial pipe locators. The depth calculated from the measured magnetic field using this proposed technique agreed within the tolerance interval representing the confidence level of 99.7% of the depth determined by the industrial devices and was able to trend changes of the buried depth. In addition, it was possible to map the target pipeline using the survey route coordinates by calculating the lateral position of the survey route relative to the pipeline centreline from the measured magnetic field. So far, the depth measured by this proposed technique has shown a potential error of 8%. By producing 3-dimensional profile of buried pipelines through quick above-ground surveys, the proposed technique can be considered as a screening technique for asset and integrity management such as monitoring geohazards conditions.

1. Introduction

Today, oil and gas pipelines are a vital part of the energy infrastructure. Monitoring and assessing a pipeline's condition is a crucial part to maintain its integrity.

For integrity management, it is beneficial for the pipeline owner to precisely know where the underground pipeline is, considering that a large part of the existing pipeline network may have bn built long ago, which may result in a lack of location data, as well as burial depth. Moreover, according to a recent report on gas pipeline incidents, the depth of buried pipelines is an important safety factor, as external interference to the pipeline is dramatically increased if the depth of cover becomes less than 80 cm [1].

‡ Corresponding author

For pipeline condition assessment, knowledge of the buried depth contributes to solving the inverse problem using recently developed large standoff magnetometry (LSM) technology [2, 3, 4], whereby stress conditions or abnormal features of the buried pipeline are determined through the remote magnetic field recorded by aboveground magnetometer surveys [5, 6, 4].

An extensive review of technologies for condition assessment of underground utilities, including pipeline locating techniques, is presented by [7]. Updates, which include techniques developed by the 10-year research program, Mapping The Underworld, can be found in [8].

The electromagnetic (or radio-frequency) techniques, in which a signal is applied to the buried pipeline using a transmitter and the induced signal of the pipeline is measured using a handheld receiver containing antennas (and/or sensors) to infer pipeline location and its burial depth [9, 10, 11], are commonly used. In practice, the location and depth of buried pipelines can be determined at individual locations using a pipe locator [12, 13]. This method usually gives a single depth measurement. Although mapping measurement locations is possible, it is a slow process when conducting long surveys.

Ground penetrating radar (GPR) transmits electromagnetic waves into the ground and employs the reflection at boundaries to detect buried structures and assess their condition [14, 15]. Thanks to radar images, GPR can be applied in positioning and mapping underground utilities, as well as in conducting condition assessment [16, 17]. Due to the greater reliance on radar images, it appears that GPR is more popular for applications in urban environments or geophysics [15, 17], where the focus is on smaller areas of tens of square meters at a time. In oil- and gas-transmission-pipeline networks, whose lengths can be tends to hundreds of kilometers, its application is more limited.

Airbone remote sensing including light detection and ranging (LIDAR) or interferometric synthetic aperture radar (InSAR) techniques can also be used to map and assess pipeline conditions on a large scale, especially in geohazardous conditions such as subsidence or landslide [18, 19, 20].

This paper introduces a passive technique to determine the depth and location of buried pipelines through the remote magnetic field of the pipeline induced by the earth's magnetic field. The proposed technique has been verified through experimental results, and its performance was evaluated during field trials against the best available technique currently used in the industry.

2. Calculation of depth and lateral position of a buried pipeline

When considering a pipeline placed in the earth's magnetic field, a horizontal plane xy above the pipeline at a distance d_m, and a three-axis magnetometer moving along the pipeline with the lateral offset to the centreline of the pipeline d_s, see Fig. 1, the angle α can be calculated as

$$\tan(\alpha) = \frac{d_s}{d_m}. \tag{1}$$

The magnetic field B_{yz} of the pipeline induced from the earth's magnetic field measured by the magnetometer when being observed along the pipe length will also be at the angle α, therefore

$$\tan(\alpha) = \frac{B_y}{B_z}. \tag{2}$$

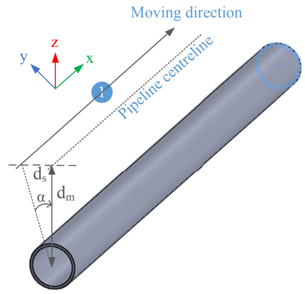

Figure 1: 3-axis fluxgate magnetometer, labelled 1, moving along the pipeline at a distance d_m and a lateral offset d_s.

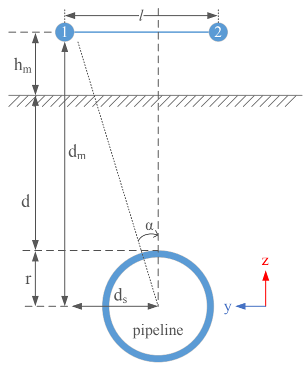

Figure 2: Schematic of the depth measurement technique.

In the case of aboveground surveys on buried pipelines, d_s is usually unknown, so to determine the distance d_m, additional measurements at another lateral offset can be performed along the pipeline. Fig. 2 shows the schematic of two measurements performed along the pipeline, labelled 1 and 2, with the pipe observed in the cross-sectional yz plane. The separation in the horizontal plane between the two measurements is l.

Given d_s is the lateral offset between a magnetometer and the centreline of the pipeline, because the distance between the measurements is l: $d_{s_1} + d_{s_2} = l$, and equation 2 applies to both measurements, the depth d_m can be calculated as

$$d_m = l/(\frac{B_{y_1}}{B_{z_1}} + \frac{B_{y_2}}{B_{z_2}}). \tag{3}$$

The lateral position of the measurement relative to the pipeline centreline, which is the offset between the magnetometer and the centreline, is

$$d_s = \frac{B_y}{B_z} d_m. \tag{4}$$

If the pipe radius r and the height of the magnetometer array above ground h_m are known, the depth of cover d can then be calculated as follows

$$d = d_m - h_m - r \tag{5}$$

Table 1: Chemical Composition of Steel Pipes

Element	Content (%)
C	≤ 0.17
Si	≤ 0.40
Mn	≤ 1.2
P	≤ 0.025
S	≤ 0.02

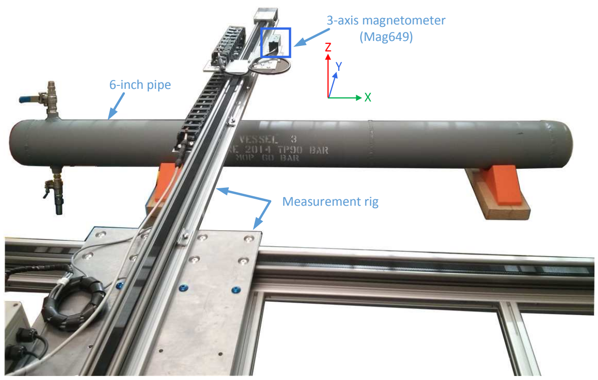

Figure 3: Experimental setup on a 6-inch 1.8 m length vessel.

3. Experiment

3.1. Experimental Setup

Experiments were performed on a 1.8-m 152-mm (6-in.) grade X42 steel vessel in the laboratory; see Table 1 for its chemical composition. A typical setup of the experiment is shown in Fig. 3.

The vessel to be tested was filled with water, pressurised up to 6 MPa (60 bar) using a hydrostatic pressure tester, and then was magnetically scanned to observe its magnetic profile of the vessel using a 3-axis fluxgate magnetometer. This was repeated at various measurement heights.

For each magnetic scan, the magnetometer was moved along the vessel by a computer-controlled rig with the magnetic field being recorded in the horizontal xy plane, taken sequentially. The same region of space was also scanned without the vessel to establish the local background magnetic field, which can then be subtracted from measurements with the vessel, to determine the true magnetic field resulting from the vessel and its operating conditions.

3.2. Experimental results

In the experiment, the magnetic field was measured along the vessel at $y = \pm 150$ mm at various heights, which was to emulate the movement of the magnetometer along the target pipeline. From the schematic shown in Fig. 2, it can be seen that when observing along the vessel length in the cross-sectional yz plane, the vector direction of the magnetic field points toward the centre of the vessel. The experimental results

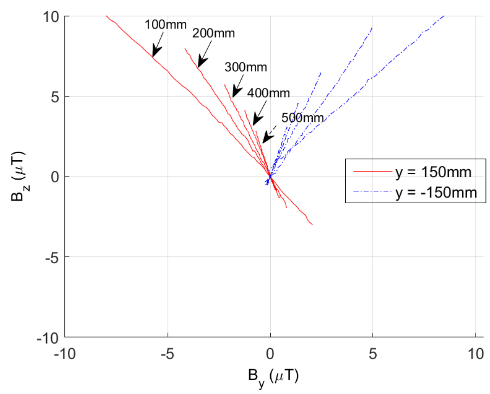

Figure 4: B_y and B_z at $y = \pm 150$ mm along the vessel versus the measurement height in yz plane.

in Fig. 4 show that when the measurement height changed from 100 mm to 500 mm, the angle of B_{yz} changed correspondingly.

Using Equation 3, the measurement height in the experiment, or the depth of burial in the case of a field survey, can be calculated from the measured magnetic field. The result shown in Fig. 5 is the height calculated from the magnetic field along with the height physically measured during the experiment. In the figure, the calculated height agreed with the measurement height of 100 mm to 300 mm. For the measurement heights of 400 mm and 500 mm, the magnitude of the magnetic field became smaller, which resulted in an error in the calculated height. In particular, the height of 410 mm and 483 mm calculated from the magnetic field related to actual measured heights of 400 mm and 500 mm, respectively. This shows an error of 2.5% and 3.4% for the respective heights.

It should be noted that, in the laboratory, as the magnetometer was mounted on a stable rig, the magnetic signal was not affected by random movements of the magnetometer, which in fact is not what normally happens in field surveys. Additionally, owing to limitations on the size of the scanning rig, the magnetometer stayed within a range where the signal strength was still detectable. Moving further away from the vessel will result in a larger error as the signal-to-noise ratio is reduced.

4. Field trial

4.1. Field surveys

Field surveys were performed on two different sections of 1,219-mm (48-in.) underground gas pipeline at the National Grid (NG) Pannal site, UK, see Fig. 6.

To collect data for the purpose of later verification, the pipeline centreline was located, and the depth from the ground level to the centre of the pipeline was recorded at regular intervals using an industrial-grade pipeline locator [12] before performing aboveground magnetic field surveys along the selected pipeline lengths. The location of all depth measurements was also recorded using a positioning system consisting of two Topcon GR-5 Global Navigation Satellite System (GNSS) receivers operating in real-time kinematic (RTK) mode [21], capable of up to 15-mm accuracy, with one receiver configured as the base station and the other configured as the mobile unit.

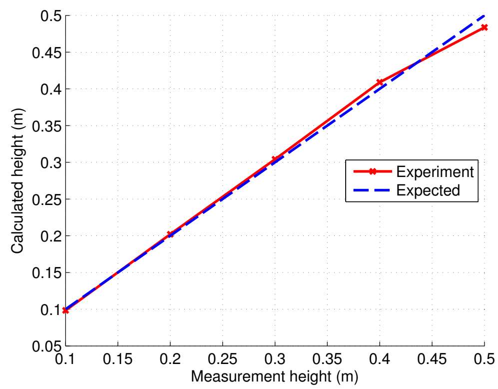

Figure 5: Comparison of the height physically measured and that calculated from the magnetic field.

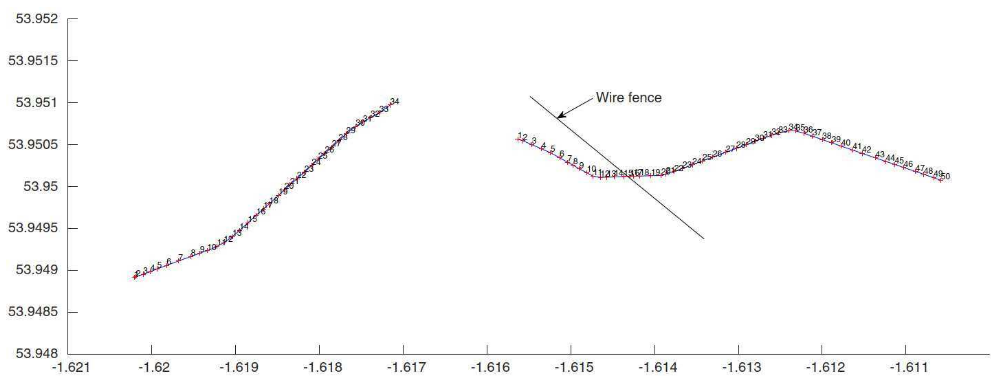

Figure 6: Map of two sections of the survey pipeline in field trials.

After mapping the pipeline, the aboveground magnetic field along the pipeline was measured four times, noted as Run 1 to Run 4, in opposite directions using a UNISCAN instrument [22]. For each run, the surveyor carried the UNISCAN instrument and walked along the pipeline centreline at a normal walking speed, approximately 0.8 m/s. The UNISCAN instrument, which was developed at the University of Leeds following requirements specified by Speir Hunter, includes an array of three-axis magnetometers and a high-accuracy positioning system. It allows the simultaneous measuring of the magnetic field at different lateral positions along the pipeline, together with the recording of the positional GNSS coordinates of each measurement [23, 24].

4.2. Field survey results

In the field surveys, the magnetic field along the pipeline behaved in a similar manner to that of the pipeline in the laboratory. As shown in Fig. 7, the vectors of the magnetic field recorded by the magnetometer array of the UNISCAN instrument along 100 m of the PANE29 pipeline directed toward the centre of the pipe, and because

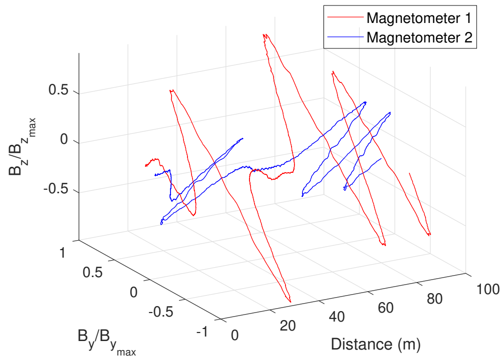

Figure 7: Magnetic field along 100 m of the PANE29 pipeline measured by the UNISCAN instrument.

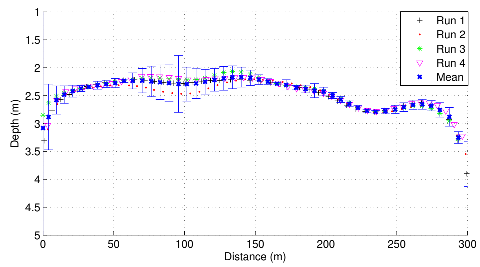

Figure 8: PANE29 section

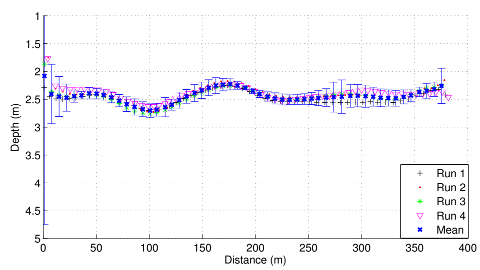

Figure 9: ASPA29 section

Figure 10: Repeatability of the depth calculated from the measured magnetic field and the mean depth.

the magnetometers were offset from the pipeline centreline, the vectors were inclined from the vertical plane.

The depth from the ground level to the centre of the pipe, calculated from the magnetic field measured during the four runs in opposite directions, is shown in Fig. 10 together with the mean depth and the tolerance interval at 95% confidence. The standard deviation of the calculated depth is shown in Fig. 13. For both of the surveyed sections, after a distance of 5 m from the start location, the calculated depth appeared to be consistent between runs with a standard deviation of 8% of the mean depth.

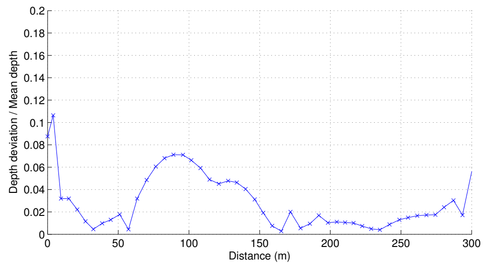

Figure 11: PANE29 section

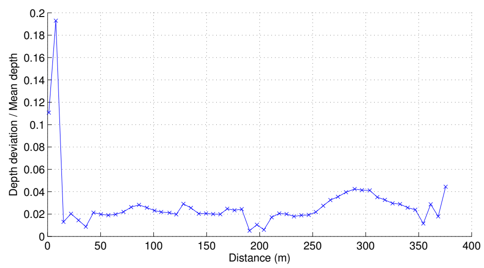

Figure 12: ASPA29 section

Figure 13: The standard deviation of the depth calculated from the measured magnetic field.

Fig. 16 compares the depth from the ground level to the centre of the pipe as determined by two different industrial pipe locators along with the mean depth calculated from the magnetic field measured by the UNISCAN instrument using Eq. 3. In the figure, the error bar of the industrial pipe locator measurements represented a range of $\pm 5\%$ with a confidence level of 99.7%.

The depth determined by the technique proposed in this paper agreed within the error bar of the measurements obtained by the industrial pipe locators for both of the surveyed sections. Additionally, it was able to trend changes in the depth reported by the pipe locators. An exception was at the distance of 120 m in the ASPA29 section, where the depth measured by the second pipe locator was at 4.5 m and the mean depth calculated by this method was approximately 2.5 m. However, it should be noted that the depth determined by the first pipe locator was also approximately 2.5 m. It is worth noting the presence of a ditch and a wire fence, see Fig. 6 between locations 11 and 15, which may have resulted in the magnetic field being incorrectly recorded for a distance of approximately 5 m in this area. In other words, there is a lower confidence in the depth calculated from the magnetic field at this location.

The offset between the magnetometer array and the pipeline centreline, which is indicated by the position of the surveyor relative to the pipeline centreline during a field survey, can be determined from the measured magnetic field using Equation 4. The results in Fig. 19 show that the surveyor was consistently above the centreline of the buried pipeline within a lateral tolerance of ± 0.1 m.

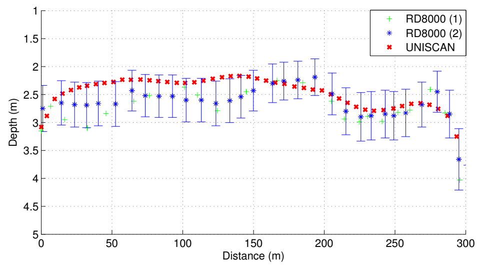

Figure 14: PANE29 section

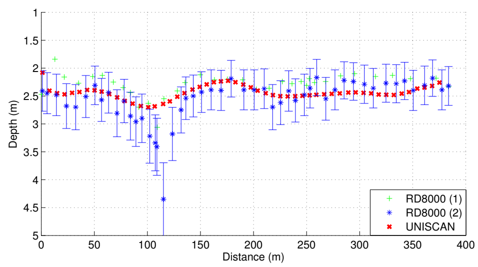

Figure 15: ASPA29 section

Figure 16: Comparison between the depths measured by the pipe locators and calculated from the measured magnetic field.

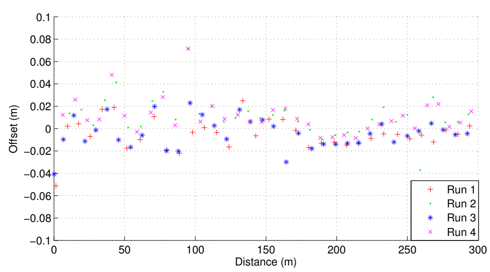

Figure 17: PANE29 section

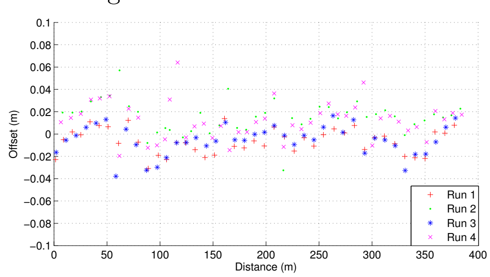

Figure 18: ASPA29 section

Figure 19: The calculated lateral offset of four runs in two opposite directions stayed within ±100 mm on top of the pipe.

5. Discussion

To verify the performance of the proposed technique during the field trials, the ideal method was to uncover and measure the buried depth of the pipelines, but it was impractical to excavate the whole pipeline. Therefore, this study used pipe locators currently used in the industry to locate the pipeline and determine the buried depth. According to the manufacturer's specification, the depth determined by the pipe locator has a standard error of 5%. An error bar of 3 standard deviations was associated with its measurements to cover the uncertainty at the confidence level of 99.7%.

Both the experimental and field survey results agreed that it is possible to employ the passive magnetic field induced by the earth's magnetic field, remotely measured by an aboveground magnetometer survey, to calculate the depth of buried pipeline using this proposed technique. For the field trial, the calculated depth agreed with the depth determined by the pipe locators, with the confidence level of 99.7%, and followed changes in the depth. This has confirmed the schematic presented in Fig. 2.

This proposed technique for determining burial depth has shown a potential error of 8%. However, this figure would require a resolution to lower confidence depth calculations caused by gaps in collected magnetic data due to obstacles along a survey route. The accuracy of the depth calculation for the first few meters of the survey route also needs to be improved.

Knowing the relative position between the survey route and the pipeline centreline allows building a three-dimensional (3D) map, which includes not only the accurate lateral position of the pipeline in terms of GNSS coordinates but also its buried depth. An accurate 3D map of underground pipelines can be useful for asset and integrity management, for example in budget estimation for excavation, or in collaborating with the owners of other assets running in close proximity. Importantly, periodically monitoring the buried depth reduces the risk of exposing the pipes running across farm lands.

Using this proposed technique to monitor ground movement such as subsidence or landslide in remote areas should also be considered. During field trials, the surveys were performed by an operator holding the instrument and continuously walking along the pipeline at normal walking speed, which was usually between 3-5 km/h. The advantage is that a survey like this can be quickly deployed with short notice. Therefore, the technique can be considered as a screening technique before deciding to deploy more expensive techniques such as tools with inertial mapping unit (IMU) [25].

It is also possible to integrate the proposed technique into other aboveground magnetic inspection techniques, including LSM, which would allow prosuction of a 3D map of the target pipeline, in addition to the inspection report.

The disadvantage is that this technique can only be applied to pipelines of ferromagnetic material. Additionally, as it measures the induced magnetic field, the signal strength depends on the magnetic property of the material. Pipe diameter is another factor that affects the induced signal strength. Results from current field surveys indicate that the technique works in case of 6-in.- and larger diameter pipelines. However, it should be noted that the pipe-diameter factor should be considered in relation to its burial depth. For example a 152-mm (6-in.) pipeline buried at a shallow depth may produce a stronger signal than a 304-mm (12-in.) pipeline buried at a deeper depth. In principle, the measured magnetic field decays in accordance to increases in burial depth, so there will be an upper limit on the measurable depth. As a guide, this limit is set between 10 to 12 times the pipe diameter; however, it needs to be investigated further in field surveys.

Because of the survey method, magnetometers of the UNISCAN instrument are subjected to noise due to random movements caused by manually handling and walking, and magnetic interference caused by nearby metallic objects. During the field trials of this work, the interference of these factors were kept to minimum by the experience operator maintaining the balance of the instrument while walking and planed to avoid metallic objects as much as possible. More controllable methods of moving the instrument during a field survey are being investigated to improve the signal quality.

6. Conclusions

This paper proposes a new technique to determine the depth and location of buried pipelines through the remote magnetic field of the pipeline without transmitting a signal to the pipe. The background calculation and the application to the laboratory experiments and field trials were presented in the paper.

It has been found that this proposed technique is capable of trending changes in burial depth over a distance, thereby determining a profile of burial depth with a potential error of 8%, verified against the best available technique used in the industry. At the same time, the pipeline can be laterally positioned from the GNSS coordinates recorded during the survey with submetre accuracy in RTK mode. Based on this, potential applications of the technique in asset and pipeline integrity management - for example, building accurate 3D profile of buried pipeline or monitoring those under geohazardous conditions - were also discussed.

Although field trials so far have shown promising results, these were derived from two different sections of pipeline, each sharing the same diameter and metallurgy. Therefore, further field surveys on different pipeline diameters and conditions should be undertaken to verify the robustness of this technique and improve the confidence level on the accuracy. This work package would also contribute to establishing a relationship between pipe diameter and its burial depth, from which upper limits of the measurable depth can be set for pipe diameters correspondingly.

Additionally, reducing movements due to walking of the magnetometers, or an upgrade in the survey procedure - for example using drones to carry the magnetometers instead of walking - would reduce uncertainties during measurements, and therefore improve the signal quality. Magnetic interference due to environmental factors, such as nearby or underground metallic objects, also needs to be explored to increase the confidence level of the reported depth - for example, suggesting a minimum distance between metallic objects and the survey route.

7. Data Availability

All data, models, and code used during the study are proprietary or confidential in nature and may only be provided with restrictions.

8. Acknowledgements

The work in this paper is possible due to the funding and support from National Grid, Speir Hunter Limited and DNV/GL.

[1] EGIG, "Gas pipeline incidents - 9th report of the european gas pipeline incident data group (period 1970 - 2013)," Feb 2015. [Online]. Available: http://www.egig.eu/uploads/bestanden/ba6dfd62-4044-4a4d-933c-07bf56b82383

[2] S. Staples, C. Vo, D. Cowell, S. Freear, C. Ives, and B. Varcoe, "Solving the inverse problem of magnetisation–stress resolution," *Journal of Applied Physics*, vol. 113, no. 13, pp. 133 905–133 905, 2013.

[3] A. Viana, L.-L. Rouve, O. Chadebec, G. Cauffet, and J.-L. Coulomb, "Inverse problem approach to characterize and model magnetization changes in a thin shell structure undergoing magneto-mechanical effects," *Magnetics, IEEE Transactions on*, vol. 47, no. 5, pp. 1450–1453, 2011.

[4] T. D. Xu, "Understanding quantitative performance of large standoff magnetometry in detecting live gas pipeline anomalies with stress estimation," in *2018 12th International Pipeline Conference*. American Society of Mechanical Engineers, 2018, pp. V001T03A020–V001T03A020.

[5] D. Atherton and D. Jiles, "Effects of stress on magnetization," *NDT international*, vol. 19, no. 1, pp. 15–19, 1986.

[6] W. Sowerbutts, "The use of geophysical methods to locate joints in underground metal pipelines," *Quarterly Journal of Engineering Geology and Hydrogeology*, vol. 21, no. 3, pp. 273–281, 1988.

[7] S. Costello, D. Chapman, C. Rogers, and N. Metje, "Underground asset location and condition assessment technologies," *Tunnelling and Underground Space Technology*, vol. 22, no. 5, pp. 524–542, 2007.

[8] T. Hao, C. Rogers, N. Metje, D. Chapman, J. Muggleton, K. Foo, P. Wang, S. R. Pennock, P. Atkins, S. Swingler *et al.*, "Condition assessment of the buried utility service infrastructure," *Tunnelling and Underground Space Technology*, vol. 28, pp. 331–344, 2012.

[9] G. T. Darilek and E. H. Cooper Jr, "Detecting buried pipeline depth and location with electromagnetic triangulation," Sep. 17 1985, uS Patent 4,542,344.

[10] A. B. Lewis, J. R. Cottle, and G. R. Cooper, "Device for locating objects that emit electromagnetic signals," Jul. 6 1999, uS Patent 5,920,194.

[11] M. S. Olsson, D. A. Cox, M. J. Martin, R. Merewether, and A. H. Jessup, "System and method for locating buried pipes and cables with a man portable locator and a transmitter in a mesh network," Sep. 11 2012, uS Patent 8,264,226.

[12] Radiodetection, "Rd8000 universal precision cable, pipe and rf marker locator range," 2014. [Online]. Available: http://www.spx.com/en/assets/pdf/RD8000brochureV10.pdf

[13] M. S. Olsson, D. E. Shaffer, R. Merewether, M. J. Martin, and D. A. Cox, "Buried object locating device with a plurality of spherical sensor balls that include a plurality of orthogonal antennae," Jun. 5 2018, uS Patent 9,989,662.

[14] D. J. Daniels, "Ground penetrating radar," *Encyclopedia of RF and Microwave Engineering*, 2005.

[15] H. M. Jol, *Ground penetrating radar theory and applications*. elsevier, 2008.

[16] D. W. Paglieroni, D. H. Chambers, S. W. Bond, and N. R. Beer, "Buried object detection in gpr images," Apr. 29 2014, uS Patent 8,711,028.

[17] W. W.-L. Lai, X. Derobert, and P. Annan, "A review of ground penetrating radar application in civil engineering: A 30-year journey from locating and testing to imaging and diagnosis," *NDT & E International*, vol. 96, pp. 58–78, 2018.

[18] C. V. Tao and Y. Hu, "Assessment of airborne lidar and imaging technology for pipeline mapping and safety applications," in *Integrated remote sensing at the global, regional and local scale, ISPRS commission I mid-term symposium in conjunction with Pecora 15/land satellite information IV conference proceedings*, 2002.

[19] M. Hornacek, D. Schall, P. Glira, S. Geiger, A. Egger, A. Filip, C. Windisch, and M. Liepe, "Geospatial analytics in the large for monitoring depth of cover for buried pipeline infrastructure," in *2018 IEEE International Conference on Cloud Engineering (IC2E)*. IEEE, 2018, pp. 233–240.

[20] R. Guthrie, E. Reid, J. Richmond, P. Ghuman, and Y. Cormier, "Insar and the pipeline geohazards toolbox: Instructions for use as of 2018," in *2018 12th International Pipeline Conference*. American Society of Mechanical Engineers, 2018, pp. V003T04A035–V003T04A035.

[21] Topcon, "Gr-5 with vanguard technology - advanced gnss receiver," 2014. [Online]. Available: https://www.topconpositioning.com/gnss/integrated-gnss-receivers/gr-5

[22] S. Hunter, "Stress concentration tomography," 2015. [Online]. Available: http://speirhunter.com/files/SCT Official Brochure.pdf

[23] S. Freear, B. Varcoe, D. M. J. Cowell, S. G. H. Staples, and C. Vo, "Fault detection

for pipelines," Sep. 6 2013, wO Patent App. PCT/GB2013/050,524. [Online]. Available: https://www.google.com/patents/WO2013128210A1?cl=en

[24] ——, "Fault detection for pipelines," Sep. 6 2013, wO Patent App. PCT/GB2013/050,526. [Online]. Available: https://www.google.com/patents/WO2013128212A1?cl=en

[25] R. Li, M. Cai, Y. Shi, Q. Feng, and P. Chen, "Technologies and application of pipeline centerline and bending strain of in-line inspection based on inertial navigation," *Transactions of the Institute of Measurement and Control*, vol. 40, no. 5, pp. 1554–1567, 2018.